Proc. Natl. Acad. Sci. USA
Vol. 93, pp. 6031–6036, June 1996
Neurobiology

The glycine binding site of the *N*-methyl-D-aspartate receptor subunit NR1: Identification of novel determinants of co-agonist potentiation in the extracellular M3–M4 loop region

(glutamate receptor/bacterial amino acid-binding protein/transmembrane topology/site-directed mutagenesis)

HIROKAZU HIRAI*, JOACHIM KIRSCH*†, BODO LAUBE*, HEINRICH BETZ*, AND JOCHEN KUHSE*‡

*Abteilung Neurochemie, Max-Planck-Institut für Hirnforschung, Deutschordenstrasse 46, 60528 Frankfurt am Main, Germany; and †Zentrum der Morphologie, Universität Frankfurt, Theodor-Stern-Kai 7, 60596 Frankfurt am Main, Germany

Communicated by Bert Sakmann, Max-Planck-Institut für Medizinische Forschung, Heidelberg, Germany, February 1, 1996 (received for review December 8, 1995)

ABSTRACT **The *N*-methyl-D-aspartate (NMDA) subtype of ionotropic glutamate receptors is a heterooligomeric membrane protein composed of homologous subunits. Here, the contribution of the M3–M4 loop of the NR1 subunit to the binding of glutamate and the co-agonist glycine was investigated by site-directed mutagenesis. Substitution of the phenylalanine residues at positions 735 or 736 of the M3–M4 loop produced a 15- to 30-fold reduction in apparent glycine affinity without affecting the binding of glutamate and the competitive glycine antagonist 7-chlorokynurenic acid; mutation of both residues caused a >100-fold decrease in glycine affinity. These residues are found in a C-terminal region of the M3–M4 loop that shows significant sequence similarity to bacterial amino acid-binding proteins. Epitope tagging revealed both the N-terminus and the M3–M4 loop to be exposed extracellularly, whereas a C-terminal epitope was localized intracellularly. These results indicate that the M3–M4 loop is part of the ligand-binding pocket of the NR1 subunit and provide the basis for a refined model of the glycine-binding site of the NMDA receptor.**

Ionotropic glutamate receptors are oligomeric ion channel proteins, which mediate fast neurotransmission at excitatory synapses in the mammalian central nervous system. Pharmacological and molecular studies have grouped these receptors into three distinct subfamilies, the α-amino-3-hydroxy-5-methyl-4-isoxazole-propionate (AMPA) receptors (subunits, GluR1-4), the kainate receptors (subunits, GluR5-7 and KA1-2), and the *N*-methyl-D-aspartate (NMDA) receptors (subunits, NR1 and NR2A-D) (1). Of these, the NMDA receptors have received particular attention, because they are implicated in both synaptic plasticity and the pathogenesis of acute and chronic neurodegenerative disorders (2-4).

A unique feature of NMDA receptors within the glutamate receptor family is their requirement for both glutamate and the co-agonist glycine for efficient gating (5, 6). Site-directed mutagenesis has identified determinants of glycine binding in both the extracellular region preceding the first membrane spanning segment M1 and the N-terminal portion of the M3–M4 loop domain of the NR1 subunit (7). From these data, a model of the binding fold composed of these two regions has been proposed (7), which is supported by significant sequence similarities between these domains of glutamate receptor subunits and a family of bacterial amino acid-binding proteins (7-9). The model implies an extracellular localization of the M3–M4 loop, which is consistent with recent studies of the transmembrane topology of mammalian AMPA and kainate receptor subunits (10-13) and the goldfish kainate binding protein (14) indicating three transmembrane segments and a reentrant membrane loop (see Fig. 1*A*, right). It differs, however, from the originally proposed topology with four transmembrane-spanning segments (see Fig. 1*A*, left) derived by analogy to other ligand-gated ion channels, such as the nicotinic acetylcholine or type A γ-aminobutyric acid receptor proteins (1, 15). The latter model is consistent with phosphorylation of different serine residues within the M3–M4 loop regions of kainate and AMPA receptor subunits both in transfected cells (16, 17) and brain slices (18).

Here, site-directed mutagenesis was used to identify novel determinants of glycine potentiation within the C-terminal portion of the M3–M4 loop of the NR1 subunit. Epitope tagging revealed that the corresponding residues are located in an extracellular domain characterized by significant sequence similarity to the bacterial lysine/arginine/ornithine binding protein (LAOBP) from *Salmonella typhimurium* (9). Based on these results, we propose a refined structural model of the co-agonist binding pocket of the NMDA receptor.

MATERIALS AND METHODS

***In Vitro* Mutagenesis.** Oligonucleotide-directed mutagenesis of the rat NR1 protein (19) was performed as described (7). For the introduction of *flag* epitopes, oligonucleotide primers of 72-bp length with a sequence encoding the *flag* domain (DYKDDDDK) were synthesized (20). *flag* epitopes were inserted into pN60 at positions following the codons corresponding to amino acid positions 375 (*flag1*), 534 (*2*), 608 (*3*), 652 (*4*), 680 (*5*), 705 (*6*), 781 (*7*), and 857 (*8*) of the NR1 protein (see Fig. 1*B*). All mutants and *flag* constructs were verified by dideoxy sequencing.

cRNA Synthesis and Oocyte Expression. Synthesis of cRNA from linearized plasmid DNA, oocyte injection, and voltage-clamp recording of the injected oocytes were performed as described (7). Dose–response curves were analyzed according to Schmieden *et al.* (21).

Cell Culture, Transfection, and Whole Cell Recording. Human 293 embryonic kidney cells (ATCC CRL1537) were cultured and transfected as described (22, 23) with equimolar amounts of cDNAs encoding wild-type or epitope-tagged NR1 and wild-type NR2B (or ε2; see ref. 24) subunits. To prevent NMDA receptor-mediated cell death, the NMDA receptor antagonist MK-801 (10 μM) was added to the culture medium after transfection (25). For electrophysiological measurements, the transfected cells were grown in the presence of the competitive glycine antagonist 7-chlorokynurenic acid (100

The publication costs of this article were defrayed in part by page charge payment. This article must therefore be hereby marked "*advertisement*" in accordance with 18 U.S.C. §1734 solely to indicate this fact.

Abbreviations: AMPA, α-amino-3-hydroxy-5-methyl-4-isoxazole-propionate; LAOBP, lysine/arginine/ornithine binding protein; NMDA, *N*-methyl-D-aspartate.

‡To whom reprint requests should be addressed.

μM). Whole-cell recordings from transfected cells were obtained as described (26).

Immunofluorescence and Confocal Microscopy. Immunolabeling of transfected cells under permeabilizing conditions was performed using a published protocol (27). For immunolabeling under nonpermeabilizing conditions, the transfected cells were incubated with the anti-FLAG M2 monoclonal antibody (Kodak) at a dilution of 1:100 (vol/vol) for 1 h. After several washes with prewarmed culture medium, the glass coverslips carrying the transfected cells were incubated for 1 h in medium containing CY3-conjugated goat anti-mouse IgG (Dianova, Hamburg, Germany; dilution, 1:500). Then, the cells were washed and fixed for 5 min in 5% (wt/vol) paraformaldehyde in phosphate-buffered saline, mounted in Mowiol (Hoechst Pharmaceuticals) and analyzed using a confocal laser scanning microscope (model Sarastro 2000, Molecular Dynamics, Sunnyvale, CA) as described (27). Transfection efficiencies were determined by calculating the ratio of immunolabeled cells under permeabilizing conditions divided by the total number of cells counted; ≈300 cells were analyzed for each of the epitope-tagged NR1 constructs. The percentage of cells immunolabeled under nonpermeabilizing conditions was determined accordingly and normalized to the efficiency of transfection. Experiments were carried out in triplicate for each determination.

RESULTS

Aromatic Amino Acid Substitutions in the M3–M4 Loop Region Alter Glycine Affinity. Comparison of the NR1 protein with periplasmic bacterial amino acid-binding proteins, in particular the glutamine-binding protein from *Escherichia coli* (28) and LAOBP (29), has revealed two regions of significant homology (7). The first corresponds to a segment in the putative extracellular domain preceding M1, and a second one is located in the amino-terminal region of the M3–M4 loop. In LAOBP, these two regions form lobes that together mediate substrate binding (29). Interestingly, the C-terminal portion of the M3–M4 loop of the NR1 subunit also displays significant homology to LAOBP (Fig. 1*C*). Because aromatic amino acids are known to be crucial for agonist binding to different neurotransmitter receptor proteins (31) including the N-terminal region of the NR1 subunit (7), the phenylalanine residues F735, F736, and F740 in this second homology region of the M3–M4 loop were replaced by nonaromatic amino acids. In addition, we mutated some of its charged amino acids as well as an arginine preceding segment M1. These NR1 mutants were then coexpressed with the NR2B subunit in *Xenopus* oocytes, and dose–response relations for glycine and glutamate were established by voltage-clamp recording.

Ion flux through the NR1/NR2B wild-type receptor was maximal at glycine concentrations between 1 and 10 μM, whereas saturation of the glutamate response occurred at 10-100 μM (Fig. 2*A*). The corresponding ligand concentrations eliciting a half-maximal current response (EC_{50}) in the presence of saturating concentrations of the second agonist were 2.8 μM for glutamate and 0.81 μM for glycine, respectively (Fig. 2 *B* and *C* and Table 1). Most of the NR1 mutants tested showed EC_{50} values for glycine and glutamate that were similar to those obtained upon coexpression of the wild-type NR1 and NR2B proteins (Table 1). However, the exchange of F735 or F736 by alanine or serine in mutants $NR1^{F735A}$, $NR1^{F735S}$, $NR1^{F736A}$, and $NR1^{F736S}$ increased the EC_{50} value for glycine by 15- to 30-fold (Fig. 2 *A* and *B*). Substitution of both residues in mutant $NR1^{F735A/F736A}$ increased the EC_{50} value of glycine by >100-fold. In contrast, the apparent glutamate affinities determined in the presence of saturating concentrations of glycine were not significantly altered by the different mutations except for mutant $NR1^{F740A}$, which showed a significant change in glutamate but not glycine affinity (Fig. 2*C* and Table 1).

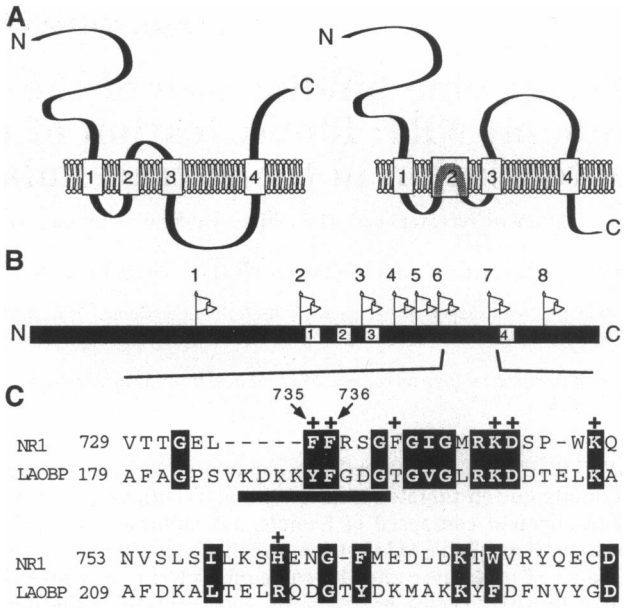

FIG. 1. Structural features of the NMDA receptor subunit NR1. (*A*) Alternative models of the transmembrane topology of glutamate receptor subunits. On the left, topology of the NR1 subunit according to Moriyoshi *et al.* (19); on the right, the three transmembrane domain model proposed for AMPA/kainate receptor subunits (11, 12). Transmembrane segments are indicated by boxes, and the reentrant membrane loop proposed for AMPA/kainate receptors is indicated by a box enclosing a U-shaped line. (*B*) Positions of *flag* epitopes in NR1 subunit constructs. Stretches of hydrophobic amino acids corresponding to putative intramembrane regions are displayed as white boxes. (*C*) Alignment of the C-terminal region of the M3–M4 loop of the NR1 subunit (19) with the corresponding sequence of LAOBP (30). Homologous residues are shown by black boxes; residues forming the second hinge region between the two lobes of the substrate binding domain of LAOBP are indicated by a horizontal black bar below the sequence. Positions where amino acid substitutions were introduced into the NR1 sequence are indicated by crosses, and mutations reducing glycine potentiation are marked by arrows. The relative position of the aligned region of the NR1 subunit is shown in *B*; amino acid numbering starts with the putative first amino acid of the mature protein (19).

Most of the substitutions did not significantly affect channel function; their maximal current responses (I_{max}) were similar to that of the wild-type NR1/NR2B protein (Table 1). However, mutants $NR1^{F735A/F736A}$ and $NR1^{K746A/T}$ showed a marked reduction in I_{max} values, and $NR1^{R505N/K}$ and $NR1^{F740S}$ never produced a detectable current upon agonist application.

We also investigated the sensitivity of the mutant receptors to the competitive glycine site antagonist 7-chlorokynurenic acid (32). Inhibition of current responses by 7-chlorokynurenic acid was not altered in the mutants $NR1^{F735A/S}$, $NR1^{F736A/S}$, and $NR1^{F735A/F736A}$ (IC_{50} values ranging from 0.69 to 0.84 μM as compared to an IC_{50} value of 0.64 ± 0.25 μM for wild-type NR1; data not shown). In contrast, the EC_{50} value of the glycine site agonist serine (5) was significantly increased for all these mutants (H.H., unpublished data). Thus, residues F735 and F736 are important determinants of glycine site agonist, but not antagonist, affinity.

Epitope Tagging Reveals an Extracellular Location of the M3–M4 Loop. To demonstrate that the region containing residues F735 and F736 is exposed extracellularly, we generated eight epitope-tagged NR1 subunit constructs (Fig. 1*B*); all contained an epitope specifically recognized by the monoclonal antibody, anti-FLAG M2 (20). The tagged NR1 subunits were coexpressed with the wild-type NR2B subunit (24) in *Xenopus* oocytes, and dose–response relations for glycine and glutamate were established by voltage-clamp recording for the resulting heterooligomeric receptors. Five of the constructs

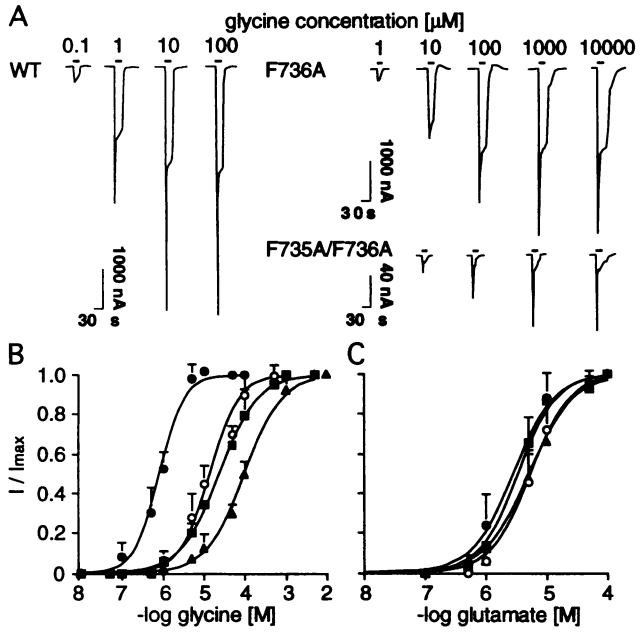

FIG. 2. Glycine responses of wild-type and mutant NR1 subunits. *In vitro*-transcribed wild-type or mutant NR1 RNAs were coinjected with the NR2B cRNA into defolliculated *Xenopus* oocytes. Membrane currents elicited by superfusion of increasing concentrations of glycine in the presence of 10 μM glutamate were recorded after 2-4 days. (*A*) Traces obtained with the wild-type NR1 subunit and the mutants $NR1^{F736A}$ and $NR1^{F735A/F736A}$ are shown. Note that the current scale for $NR1^{F735A/F736A}$ differs from those of the other recordings. (*B* and *C*) Agonist dose–response curves of wild-type and mutant NR1 subunits coexpressed with NR2B. Dose–response curves for glycine in the presence of a saturating concentration of glutamate (*B*) and for glutamate in the presence of a saturating concentration of glycine (*C*) were determined for the wild-type NR1 (●) and the mutant $NR1^{F735A}$ (○), $NR1^{F736A}$ (■), and $NR1^{F735A/F736A}$ (▲) subunits. For EC_{50} values, see Table 1.

tested displayed a glycine and glutamate pharmacology resembling that of the wild-type NR1 subunit (Table 2). Three constructs (NR1-*flag2*, NR1-*flag3*, and NR1-*flag6*) did not yield agonist-induced currents under our experimental conditions. Coexpression of the constructs NR1-*flag1*, NR1-*flag5*, and NR1-*flag8* with the NR2B subunit in the human embryonic kidney cell line 293 also generated agonist-gated ion channels (data not shown). Again, no significant differences between epitope-tagged and wild-type NR1 subunits could be detected.

The transmembrane topology of the epitope-tagged NR1 subunit was visualized by immunolabeling of cells coexpressing the NR1 constructs and the wild-type NR2B subunit. Immunolabeling under permeabilizing conditions revealed that all epitope-tagged NR1-*flag* constructs were localized at the cell membrane in large immunoreactive clusters of about 2.7 ± 2.1 μm^2 (mean ± SD, $n = 113$; see Fig. 3, *Left*; data not shown). When the cells were immunolabeled under nonpermeabilizing conditions, however, only the epitope tags located at the N-terminus (NR1-*flag1*) and between the transmembrane segments M3 and M4 (NR1-*flag4*, NR1-*flag5*, NR1-*flag6*, and NR1-*flag7*) were exposed at the surface of the transfected cells (Fig. 3, *Right*; data not shown). In contrast, epitope tags located at the N-terminus close to the postulated first transmembrane region (NR1-*flag2*), at the position preceding segment M3 (NR1-*flag3*), and at the C-terminus (NR1-*flag8*) were not detected in nonpermeabilized cells, although bright immunostaining was seen upon permeabilization (Fig. 3, *Bottom*; data not shown). This is consistent with an intracellular location of the *flag3* and *flag8* epitopes; the inaccessibility of the epitope preceding M1 (NR1-*flag2*) in nonpermeabilized cells may be due to its proximity to the lipid bilayer.

Table 1. Agonist responses of the NR1 mutants

Mutant	EC_{50}, μM		I_{max}, μA	*n*
	L-Glutamate	Glycine		
NR1	2.8 ± 1.2	0.81 ± 0.32	3.7 ± 1.3	7
R505N	–	–	NF	10
R505K	–	–	NF	10
F735A	5.1 ± 1.0	13 ± 3.8*	3.6 ± 0.9	4
F735S	6.5 ± 1.4	19 ± 5.9*	2.2 ± 0.7	4
F736A	3.4 ± 1.5	23 ± 3.5*	1.2 ± 0.4	4
F736S	2.0 ± 1.1	22 ± 7.4*	6.8 ± 2.5	5
F735A/F736A	5.4 ± 1.5	96 ± 7.5*	0.15 ± 0.04	3
F740A	10.4 ± 3.3*	1.0 ± 0.5	4.5 ± 0.6	4
F740S	–	–	NF	10
K746A	ND	ND	0.04 ± 0.03	10
K746T	4.6 ± 0.3	1.1 ± 0.1	0.14 ± 0.05	2
D747H	2.7 ± 0.2	2.4 ± 0.7	3.1 ± 0.5	4
D747Y	3.2 ± 0.3	3.0 ± 0.8	5.3 ± 1.0	4
K751M	1.8 ± 0.4	0.90 ± 0.51	3.7 ± 1.1	4
H762P	5.4 ± 0.2	0.83 ± 0.43	3.2 ± 1.8	4

NR1 wild-type and mutant cRNAs were coinjected with the NR2B cRNA into *Xenopus* oocytes, and the receptors generated were analyzed by voltage-clamp recording as detailed. EC_{50} values ± SD were calculated from dose–response curves obtained from *n* oocytes each. I_{max} values were determined in the presence of saturating concentrations of both L-glutamate and glycine. ND, not determined; and NF, nonfunctional.

*Statistically significant changes as compared to the EC_{50} value of the wild-type receptor (two-tailed *t*-test, $P < 0.01$).

Quantitative evaluation of the immunocytochemical data substantiated these findings. Of the transfected cells coexpressing NR2B with NR1-*flag1*, NR1-*flag5*, or NR1-*flag6*, 75-92% displayed surface labeling under nonpermeabilizing conditions, whereas only a very low percentage (4.0 ± 0.3%) of cells was weakly immunoreactive in cultures coexpressing NR2B with NR1-*flag8*. We therefore conclude that in heterooligomeric NMDA receptors both the N-terminus and the entire M3–M4 loop of the NR1 polypeptide are extracellular, whereas the C-terminus extends into the interior of the cell.

DISCUSSION

Our data demonstrate the extracellular localization of the M3–M4 loop of the NR1 subunit and disclose novel determinants of glycine binding in this region. Substitution of residues F735 or F736 in the C-terminal half of the M3–M4 loop caused a significant decrease in apparent glycine affinity without

Table 2. Agonist responses of the NR1-*flag* constructs

Construct	EC_{50}, μM	
	L-Glutamate	Glycine
NR1	2.8 ± 1.2	0.81 ± 0.32
NR1-*flag1*	1.8 ± 0.7	0.60 ± 0.31
NR1-*flag2*	NF	NF
NR1-*flag3*	NF	NF
NR1-*flag4*	3.3 ± 0.7	1.4 ± 0.3
NR1-*flag5*	2.3 ± 1.1	0.70 ± 0.25
NR1-*flag6*	NF	NF
NR1-*flag7*	2.4 ± 0.5	0.93 ± 0.34
NR1-*flag8*	3.1 ± 1.0	1.2 ± 0.4

EC_{50} values were obtained from *Xenopus* oocytes coinjected with cRNA synthesized from the various construct and the NR2B cDNAs using two-electrode voltage-clamp conditions. For the determination of glutamate and glycine dose–response curves, glycine or glutamate were coapplied at saturating concentrations of 10 and 100 μM, respectively. NF, nonfunctional.

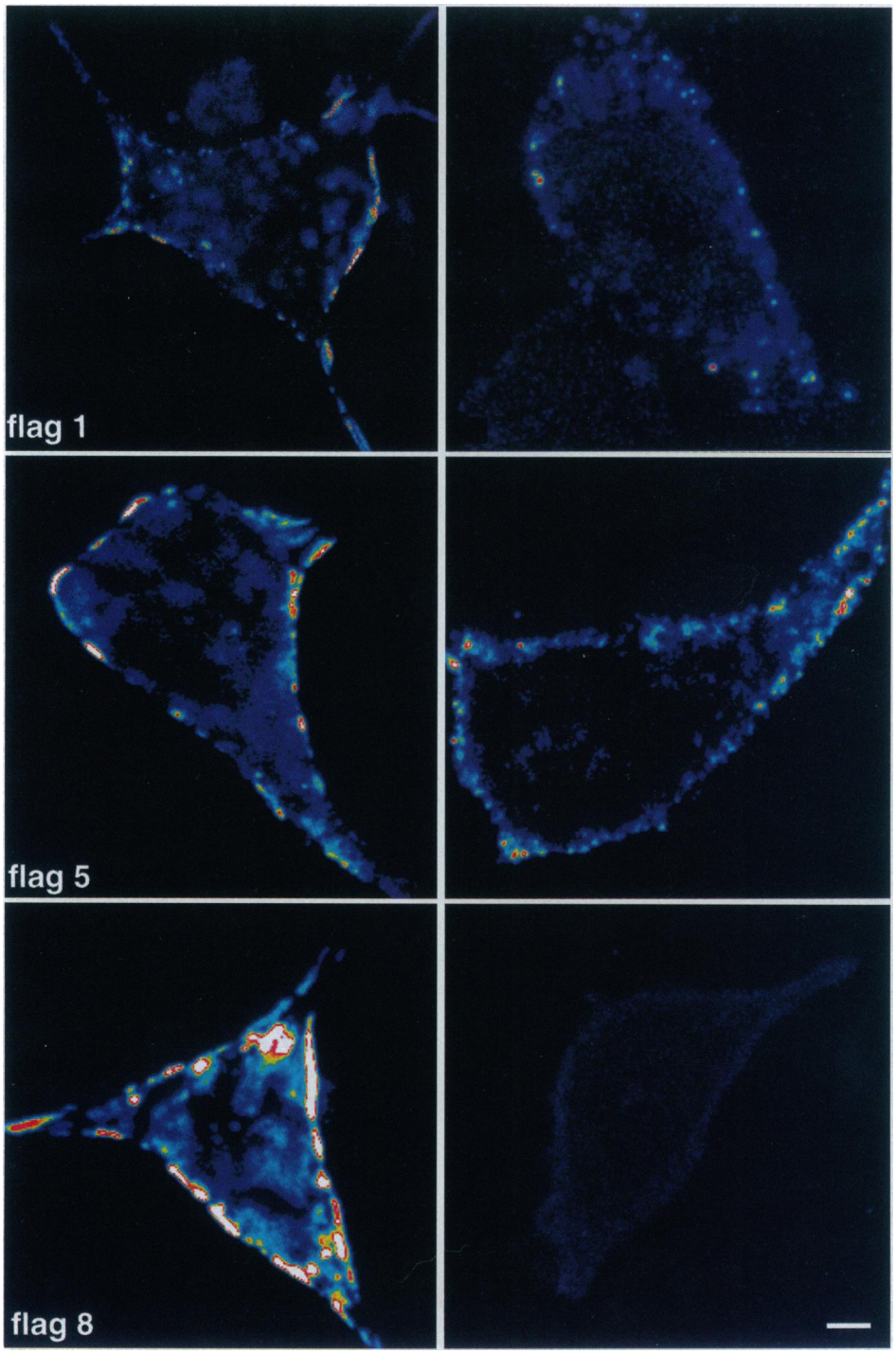

FIG. 3. Confocal optical sections of 293 cells coexpressing epitope-tagged NR1 and wild-type NR2B subunits. Coverslip cultures of transfected cells were processed for immunolabeling with the anti-FLAG M2 monoclonal antibody under permeabilizing (*Left*) and nonpermeabilizing (*Right*) conditions. Immunostaining under permeabilizing conditions (*Left*) shows the presence of the epitope-tagged NR1 constructs NR1-*flag1*, NR1-*flag5*, and NR1-*flag8* at the plasma membrane. Note the discontinuous distribution of NR1 immunoreactivity. Immunolabeling under nonpermeabilizing conditions (*Right*) reveals the N-terminal *flag1* epitope (*Top*) and *flag5* in the M3–M4 loop (*Middle*); the C-terminal epitope *flag8* (*Bottom*), in contrast, is not detected, although the respective polypeptide is expressed at the plasma membrane (*Bottom left*). Bar = 5 μm.

changing the glutamate response. This effect was potentiated upon exchanging both amino acids with alanine, whereas other mutations in this region had no effect. Moreover, total membrane currents were significantly reduced in the double mutant $NR1^{F735A/F736A}$, indicating that channel gating might be impaired. As mentioned above, significant homologies exist between glutamate receptor proteins and periplasmic bacterial amino acid-binding proteins, such as the glutamine-binding protein and LAOBP (7-9, 28). The three-dimensional structure of LAOBP with and without bound ligand has been solved by x-ray crystallography; this revealed a binding pocket formed from two lobular domains connected by two short peptide "hinge" regions (first and second connecting strands; see ref. 29). These hinge regions allow for rotational movement to generate "open" and "closed" conformations of LAOBP. When a ligand binds to the first lobe, the two lobes come in contact with each other, and the closed conformation is stabilized (29).

Residues F735 and F736 of the NR1 protein correspond to Y190 and F191, respectively, in the second connecting strand of LAOBP (see Fig. 1*C*). Y190 in LAOBP is one of the key residues allowing for the opening and closing of the ligand binding pocket by generating a large torsion between Y190 and K189 (29). In LAOBP, neither of the connecting strands between the lobes interacts with the substrate; however, hydrogen bonds established between the residues in these "connectors" are thought to contribute to the three-dimensional structure of the ligand-binding pocket and to play an important role for the dynamic movement of the lobes (29). Assuming that the hinge structure of the ligand binding pocket of LAOBP is conserved in the NMDA receptor, the decrease in glycine affinity found with our mutants $NR1^{F735A/S}$, $NR1^{F736A/S}$, and $NR1^{F735A/F736A}$ may result from an altered tertiary structure of the ligand-binding pocket that is caused by a disruption of the hydrogen bond network in the hinge region. Consistent with this view, many mutations of the NR1 subunit ($NR1^{F515A}$, $NR1^{Y517S}$, and $NR1^{V524A/I}$) located at or close to a stretch of amino acids (positions 517-520) that can be aligned to the first connecting strand of LAOBP showed low or no channel function upon heterologous expression (7).

Previous mutations of aromatic residues in the NR1 protein, $NR1^{F390S/W}$, $NR1^{Y392A}$, and $NR1^{F466A/H}$, which correspond to residues in lobe 1 of LAOBP (see Fig. 4), all drastically increased the IC_{50} value of 7-chlorokynurenic acid (7). In contrast, the mutants $NR1^{F735A/S}$, $NR1^{F736A/S}$, and $NR1^{F735A/F736A}$ analyzed here did not show a significant change in 7-chlorokynurenic acid inhibition. This suggests that the 7-chlorokynurenic acid-binding site may be exclusively located on the putative lobe 1 region of the NR1 protein and that binding of the antagonist to this region may prevent the closing movement of the ligand-binding pocket by steric hindrance.

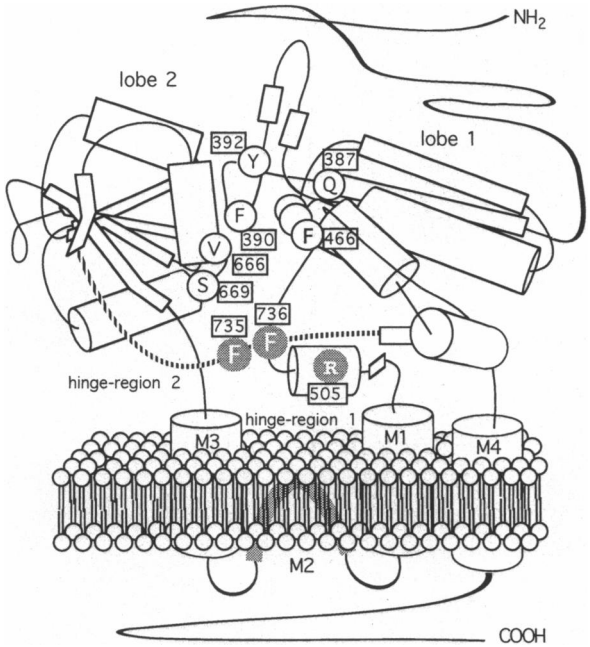

FIG. 4. Model of the transmembrane topology and glycine-binding pocket of the NR1 subunit. The NR1 substitutions affecting glycine affinity revealed in this (●) and a previous (○) study (7) are projected schematically into the three-dimensional structure of LAOBP (29). In this model, the membrane segments M1–M3 are replacing the hinge region 1 of LAOBP, which connects lobes 1 and 2. The putative hinge region 2 indicated by a dotted line contains residues F735 and F736 identified here as determinants of glycine binding. The amino acid sequences connecting lobes 1 and 2 to transmembrane segments, as well as the N- and C-terminal extensions of NR1, are not represented at scale. The M2 region is drawn as a membrane reentrant loop as proposed for the AMPA receptors (11, 12).

Substitution of arginine 505 of the NR1 protein by asparagine or lysine also abolished the agonist response. In LAOBP, the homologous residue R77 is used to stabilize the ligand's carboxyl group (29). In the GluR1 protein, substitution of the corresponding residue R481 results in a loss of receptor function (33). These data suggest that the conserved arginine at position 505 of the NR1 protein (Fig. 4) may be directly involved in glycine binding.

Immunocytochemical analysis of the expressed epitope tags confirmed the extracellular localization of the M3–M4 loop. In addition, our data are consistent with a topology characterized by an extracellular N-terminus and an intracellular C-terminus, respectively. The inaccessibility of the C-terminal epitope tag of NR1-*flag8* in nonpermeabilized cells cannot be attributed to the retention of misfolded polypeptides in the endoplasmic reticulum; as in permeabilized cells, this tagged NR1 subunit was seen at the plasmamembrane. Also, the NR1-*flag8* construct formed functional receptors that resembled those generated with the wild-type NR1 subunit. Thus, our data show that the transmembrane topology model previously established for AMPA and kainate receptor proteins (Fig. 1*A*, Right; see refs. 10-14) also holds for the NMDA receptor subunit NR1. Independent support comes from studies demonstrating phosphorylation of serines within the C-terminal tail of the NR1 protein (34) and use of a N-glycosylation consensus site engineered into its M3–M4 loop sequence (35).

In conclusion, these and our previous (7) results show that several residues along the M3–M4 loop domain are essential for glycine potentiation. These residues are localized extracellularly in regions displaying significant sequence similarity with LAOBP, thus supporting a model of the glycine-binding fold based on the bilobular three-dimensional structure of LAOBP. This model should foster the rational design of drugs that target this site and thus might be suitable for the prevention of neurodegenerative disorders caused by pathological activation of this ligand-gated ion channel.

We thank Drs. S. Nakanishi and M. Mishina for supplying the NR1 and NR2B cDNAs, D. Magalei and J. Lorentz for technical assistance, and M. Baier and H. Reitz for secretarial help. This work was supported by Deutsche Forschungsgemeinschaft (SFB 169, Schwerpunktprogramm "Funktionelle Domänen", and Ki339/4-2), Human Capital and Mobility Program (ERBCHRXCT930167), and Fonds der Chemischen Industrie. H. Hirai and B. Laube hold Max-Planck postdoctoral fellowships, and J. Kirsch is the recipient of a Heisenberg fellowship of the Deutsche Forschungsgemeinschaft.

1. Seeburg, P. H. (1993) *Trends Neurosci.* **16,** 359–365.
2. Choi, D. W. (1988) *Neuron* **1,** 623–634.
3. Madison, D. V. (1991) *Annu. Rev. Neurosci.* **14,** 379–397.
4. Bliss, T. V. & Collingridge, G. L. (1993) *Nature (London)* **361,** 31–39.
5. Johnson, J. W. & Ascher, P. (1987) *Nature (London)* **325,** 529–531.
6. Kleckner, N. W. & Dingledine, R. (1988) *Science* **241,** 835–837.
7. Kuryatov, A., Laube, B., Betz, H. & Kuhse, J. (1994) *Neuron* **12,** 1291–1300.
8. Nakanishi, N., Shneider, N. A. & Axel, R. (1990) *Neuron* **5,** 569–581.
9. O'Hara, P. J., Sheppard, P.-O., Thøgersen, H., Venezia, D., Haldemann, B. A., McGrane, V., Houamed, K. M., Thomsen, C., Gilber, T. L. & Mulvihill, E. R. (1993) *Neuron* **11,** 41–52.
10. Kuusinen, A., Arvola, M. & Keinänen, K. (1995) *EMBO J.* **14,** 6327–6332.
11. Hollmann, M., Maron, C. & Heinemann, S. (1994) *Neuron* **13,** 1331–1343.
12. Bennett, J. A. & Dingledine, R. (1995) *Neuron* **14,** 373–384.
13. Stern-Bach, Y., Bettler, B., Hartley, M., Sheppard, P. O., O'Hara, P. J. & Heinemann, S. F. (1994) *Neuron* **13,** 1345–1357.

14. Wo, Z. G. & Oswald, R. E. (1995) *J. Biol. Chem.* **270,** 2000–2009.
15. Stroud, R. M., McCarthy, M. P. & Shuster M. (1990) *Biochemistry* **29,** 11009–11023.
16. Raymond, L. A., Blackstone, C. D. & Huganir, R. L. (1993) *Nature (London)* **361,** 637–641.
17. Wang, L. Y., Taverna, F. A., Huang, X. P., MacDonald, J. F. & Hampson, D. R. (1993) *Science* **259,** 1173–1175.
18. Nakazawa, K., Mikawa, S., Hashikawa, T. & Ito M. (1995) *Neuron* **15,** 697–709.
19. Moriyoshi, K., Masu, M., Ishii, T., Shigemoto, R., Mizuno, N. & Nakanishi, S. (1991) *Nature (London)* **354,** 31–37.
20. Power, B. E., Ivancic, N., Harley, V. R., Webster, R. G., Kortt, A. A., Irving, R. A. & Hudson, P. J. (1992) *Gene* **113,** 95–99.
21. Schmieden, V., Grenningloh, G., Schofield, P. R. & Betz, H. (1989) *EMBO J.* **8,** 695–700.
22. Kirsch, J., Kuhse, J. & Betz, H. (1995) *Mol. Cell. Neurosci.* **6,** 450–461.
23. Chen, C. & Okayama, H. (1987) *Mol. Cell. Biol.* **7,** 2745–2751.
24. Kutsuwada, T., Kashiwabuchi, N., Mori, H., Sakimura, K., Kushiya, E., Araki, K., Meguro, H., Masaki, H., Kumanishi, T., Arakawa, M. & Mishina, M. (1992) *Nature (London)* **358,** 36–41.
25. Anegawa, N. J., Lynch, D. R., Verdoorn, T. A. & Pritchett, D. B. (1995) *J. Neurochem.* **64,** 2004–2012.
26. Bormann, J., Rundström, N., Betz, H. & Langosch, D. (1993) *EMBO J.* **12,** 3729–3737.
27. Kirsch, J. & Betz, H. (1995) *J. Neurosci.* **15,** 4148–4156.
28. Nohno, T., Saito, T. & Hong, J.-S. (1986) *Mol. Gen. Genet.* **205,** 260–269.
29. Oh, B.-H., Pandit, J., Kang, C.-H., Nikaido, K., Gokcen, S., Ames, G. F.-L. & Kim, S. H. (1993) *J. Biol. Chem.* **268,** 11348–11355.
30. Kang, C.-H., Shin, W.-C., Yamagata, Y., Gokcen, S., Ames, G. F.-L. & Kim, S.-H. (1991) *J. Biol. Chem.* **266,** 23893–23899.
31. Galzi, J.-L. & Changeux, J.-P. (1994) *Curr. Opin. Struct. Biol.* **4,** 554–565.
32. Kemp, J. A., Foster, A. C., Leeson, P. D., Priestley, T., Tridgett, R., Iversen, L. L. & Woodruff, G. N. (1988) *Proc. Natl. Acad. Sci. USA* **85,** 6547–6550.
33. Uchino, S., Sakimura, K., Nagahari, K. & Mishina, M. (1992) *FEBS Lett.* **308,** 253–257.
34. Tingley, W. G., Roche, K. W., Thompson, A. K. & Huganir, R. L. (1993) *Nature (London)* **364,** 70–73.
35. Wood, M. W., VanDongen, H. M. A. & VanDongen, A. M. J. (1995) *Proc. Natl. Acad. Sci. USA* **92,** 4882–4886.